Intramolecular Singlet and Triplet Energy Transfer in a Ruthenium(II) Diimine Complex Containing Multiple Pyrenyl Chromophores

Daniel S. Tyson and Felix N. Castellano*

Department of Chemistry and Center for Photochemical Sciences, Bowling Green State University, Bowling Green, Ohio 43403

Received: August 23, 1999; In Final Form: October 7, 1999

We report the synthesis and the photophysical properties of UV light-harvesting arrays constructed around a $[Ru(bpy)_3]^{2+}$ core (bpy = 2,2′-bipyridine) bearing one and three pyrenyl units in the periphery. The free ligand containing the pyrenyl unit, 4-methyl-4′-(2-hydroxyethylpyrenyl)-2,2′-bipyridine, displays an intense emission band centered near 400 nm with a lifetime of 264 ns, characteristic of singlet pyrene emission. The complexes $[Ru(dmb)_2$(4-methyl-4′-(2-hydroxyethylpyrenyl)-2,2′-bipyridine)$](PF_6)_2$, where dmb is 4,4′-dimethyl-2,2′-bipyridine, and $[Ru($4-methyl-4′-(2-hydroxyethylpyrenyl)-2,2′-bipyridine$)_3](PF_6)_2$ exhibit visible emission characteristic of the $[Ru(bpy)_3]^{2+}$ unit, regardless of excitation wavelength. The singlet emission from the pyrene chromophores is almost quantitatively quenched by the metal-to-ligand charge transfer (MLCT) states of each respective Ru(II) complex resulting in the observation of sensitized MLCT-based emission. On account of the energetic proximity between the ^{3}MLCT states and the ^{3}pyrene states, a long-lived ^{3}MLCT emission is observed which decays with the same first-order lifetime as the pyrene triplet states in deaerated CH_3CN. In deaerated CH_3CN, the bichromophoric system displays a lifetime of 2.96 μs, whereas the tetrad complex exhibits a lifetime of 9.0 μs. The results are indicative of excited-state equilibrium between the ^{3}MLCT and ^{3}pyrene states. Our findings demonstrate rapid and efficient singlet−singlet energy transfer through the antenna effect whereas the reversible triplet−triplet energy transfer processes help sustain long-lived MLCT excited states.

Introduction

Recently, there has been a significant effort dedicated to the study of bichromophores consisting of a Ru(II) diimine complex that displays metal-to-ligand charge transfer (MLCT) excited states[1] and a covalently linked pyrene molecule.[2−5] In cases where the two chromophores are separated by an alkyl tether, reversible triplet−triplet energy transfer occurs between the ^{3}pyrene and the ^{3}MLCT excited states.[2,3] Consequently, the observed ^{3}MLCT-based emission is substantially longer lived (up to 11-fold) as a result of the stabilization imparted by the equilibrium process. When there is no spacer group between the diimine ligand and the pyrene unit or when the spacer is an alkynyl linker, the ^{3}MLCT lifetimes become extremely long (approaching 50 μs).[4,5] The lifetimes in these dyads are modulated in part by the spacer but are ultimately controlled by the relative triplet energy levels of the two chromophores. In addition to these interesting triplet−triplet processes, it has been shown that singlet−singlet energy transfer between the pyrene moiety and the Ru(II) MLCT complex is also efficient.[3] This has been demonstrated through the intramolecular quenching of the ^{1}pyrene emission and the close match of the excitation and absorption spectra of the bichromophore.[3] These results suggest the singlet−singlet energy transfer strategies traditionally employed in artificial light-harvesting arrays can be adapted to incorporate MLCT excited states. We have recently explored this possibility by using multiple coumarin donor molecules in conjunction with a single Ru(II) MLCT complex acceptor.[6] The coumarin-containing UV light-harvesting arrays exclusively produce long-lived MLCT-based emission, regardless of excitation wavelength. A similar approach has been recently taken to harvest UV photons below 300 nm through the use of multiple naphthalene units arranged around a $[Ru(bpy)_3]^{2+}$ core.[7]

The present work combines the facets of singlet−singlet and triplet−triplet processes within the same molecule in order to generate efficient light-harvesting systems that display long lifetime emission. Such molecules are of interest for luminescence-based analytical applications[8] and for molecular device research.[9,10] We prepared two molecules which incorporate either one (dyad) or three (tetrad) pyrene molecules covalently linked through alkyl tethers to a single ruthenium(II) diimine MLCT complex. UV excitation of the pyrenyl antennae results in rapid and efficient singlet−singlet energy transfer to the $[Ru(bpy)_3]^{2+}$ core, generating a sensitized MLCT-based emission. The intervening pyrene triplet states that are nearly isoenergetic with the ^{3}MLCT states prolong the MLCT-based emission to 2.96 μs in the dyad and to 9.0 μs in the tetrad at room temperature. The extended lifetimes in these compounds are described by an excited-state equilibrium between the triplet states of the pyrene unit(s) and the Ru(II) MLCT core complex.

Experimental Section

General Data. All manipulations were performed under an inert and dry argon atmosphere using standard techniques. Anhydrous THF, 2,2′-bipyridine (bpy), 4,4′-dimethyl-2,2′-bipyridine (dmb), *n*-butyllithium (1.6 M in hexanes), and 1-pyrenecarboxaldehyde were obtained from Aldrich and used as received. Diisopropylamine (Aldrich) was distilled from CaH_2 immediately before use. Water was deionized with a Barnstead E-Pure system. All other reagents and materials from com-

* Corresponding author. E-mail: castell@bgnet.bgsu.edu.

10.1021/jp992983w CCC: $18.00
Published on Web 11/12/1999

mercial sources were used as received. $Ru(dmb)_2Cl_2$,[11] $Ru(DMSO)_4Cl_2$,[12] and $[Ru(dmb)_3](PF_6)_2$[13] were prepared according to published procedures. Commercially available $[Ru(bpy)_3]Cl_2 \cdot 6H_2O$ (Aldrich) was converted into the corresponding PF_6 salt by metathesis with NH_4PF_6 (Aldrich) in water. Column chromatography used neutral alumina (Aldrich). Reversed-phase HPLC was performed with a Hewlett-Packard HPLC system equipped with a diode array absorption detector.

^1H NMR spectra were recorded on a Varian Gemini 200 (200 MHz) spectrometer. All chemical shifts are referenced to residual solvent signals previously referenced to TMS. FAB mass spectra were measured at the University of Maryland, College Park, Mass Spectrometry Laboratory. Elemental analyses were obtained at the Analytical Facilities, University of Toledo.

Syntheses. 4-Methyl-4′-(2-hydroxyethylpyrenyl)-2,2′-bipyridine (bpy-pyrene). *n*-Butyllithium (17.5 mL, 28 mmol) in hexanes was added to a solution of diisopropylamine (4 mL, 28.5 mmol) in dry THF (150 mL) at −78 °C under argon. The pale yellow solution of LDA was stirred at −78 °C for 30 min, and then a solution of dmb (5.0 g, 27 mmol) in dry THF (150 mL) was added dropwise via cannula to produce a dark orange-red solution. The dry ice acetone bath was then replaced with an ice−water bath, and the mixture was stirred for 1 h at 0 °C. A solution of 1-pyrenecarboxyaldehyde (6.91 g, 30 mmol) in 100 mL dry THF was then added dropwise via cannula. The solution turned dark yellow near the end of the aldehyde addition. Stirring was continued for 1 h at 0 °C and then at ambient temperature for 1 h. The reaction was quenched with methanol (5 mL) and then poured into water (100 mL) and extracted with $CHCl_3$ (3 × 100 mL). The combined organic extracts were dried over Na_2SO_4, filtered, and rotary evaporated to dryness (8.8 g). The crude product was recrystallized from 350 mL of hot CH_2Cl_2. The solid was collected by vacuum filtration on a Buchner funnel and washed with 100 mL of CH_2Cl_2. The white solid was dried at room temperature in the dark (4.2 g, 38% yield). Anal. Calcd for $C_{29}H_{22}N_2O \cdot 0.5CH_2Cl_2$: C, 77.53; H, 5.07; N, 6.13. Found: C, 78.14; H, 5.05; N, 6.19. ^1H NMR ($CDCl_3$): δ 2.44 (s, 3H), 3.39 (m, 2H), 6.12 (q, 1H), 7.18 (quartet of doublets, 2H), 8−8.25 (bm, 9H), 8.39 (s, 1H), 8.41 (d, 1H), 8.55 (t, 2H). MS (FAB): *m*/*z* 415 $M - H^+$.

Bis(4,4′-dimethyl-2,2′-bipyridine)[4-methyl-4′-(2-hydroxyethylpyrenyl)-2,2′-bipyridine]ruthenium(II) Hexafluorophosphate, $[Ru(dmb)_2(bpy\text{-}pyrene)](PF_6)_2$. $Ru(dmb)_2Cl_2$ (26 mg, 0.085 mmol) and 4-methyl-4′-(2-hydroxyethylpyrenyl)-2,2′-bipyridine (38.9 mg, 0.094 mmol) were suspended in methanol (40 mL), protected from light, and refluxed for 3 h while being stirred under Ar. The reaction solution was cooled to room temperature and filtered, and water (10 mL) was added to the filtrate. Dropwise addition of 20 mL of saturated NH_4PF_6(aq) generated a bright orange precipitate. The precipitate was collected by vacuum filtration through a fine glass frit and washed with water, followed by diethyl ether to afford the crude orange product (75 mg). The solid was purified by chromatography on alumina (1:1 CH_3CN:toluene) and recrystallized by addition of NH_4PF_6(aq) to a concentrated CH_3CN solution of the complex (60 mg, 60% yield). The complex was further purified by reversed-phase HPLC (C-18). Anal. Calcd for $C_{53}H_{46}N_6ORuP_2F_{12} \cdot 6H_2O$: C, 49.65; H, 4.55; N, 6.55. Found: C, 49.54; H, 3.91; N, 6.56. MS (FAB): *m*/*z* 1029.5 $[M - PF_6]^+$, 884.4 $[M - 2PF_6]^{2+}$.

Tris(4-methyl-4′-(2-hydroxyethylpyrenyl)-2,2′-bipyridine)ruthenium(II) Hexafluorophosphate, $[Ru(bpy\text{-}pyrene)_3](PF_6)_2$. $Ru(DMSO)_4Cl_2$ (102.7 mg, 0.212 mmol) and 4-methyl-4′-(2-hydroxyethylpyrenyl)-2,2′-bipyridine (129 mg, 0.7 mmol) were dissolved in 95% ethanol (10 mL), protected from light, and refluxed for 24 h under Ar. This solution was cooled to room temperature, 5 mL of H_2O was added, and the mixture was filtered. Excess NH_4PF_6(aq) was added, and a red-brown solid immediately precipitated. The precipitate was filtered through a fine glass frit and washed with water and ether to afford the crude red-brown product (171 mg, 86% yield). The complex was purified by reversed-phase HPLC (C-18). Anal. Calcd for $C_{87}H_{66}N_6O_3RuP_2F_{12} \cdot 3H_2O$: C, 61.88; H, 4.29; N, 4.97. Found: C, 61.15; H, 3.85, N, 5.07. MS (FAB): *m*/*z* 1489.2 $[M - PF_6]^+$, 1345.1 $[M - 2PF_6]^{2+}$.

Physical Measurements. Absorption spectra were measured with a Hewlett-Packard 8453 diode array spectrophotometer, accurate to ±2 nm. Static luminescence spectra were obtained with a single photon counting spectrofluorimeter from Edinburgh Analytical Instruments (FL/FS 900). The temperature in the fluorimeter was maintained at 25 ± 1 °C for all measurements with a Neslab RTE−111 circulating bath. The excitation was accomplished with a 450W Xe lamp optically coupled to a monochromator (±2 nm), and the emission was gathered at 90° and passed through a second monochromator (±2 nm). The luminescence was measured with a Peltier-cooled (−30°C), R955 red-sensitive photomultiplier tube (PMT). Excitation spectra were corrected with a photodiode mounted inside the fluorimeter that continuously measures the Xe lamp output. This instrument was also utilized for time-correlated single photon counting (TCSPC) experiments. The excitation source for the TCSPC measurements was a nanosecond flashlamp operating under an atmosphere of H_2 gas (0.50−0.55 bar, 0.7 nm fwhm, 40 kHz repetition rate), whose output was filtered through a monochromator prior to sample excitation. TCSPC data were analyzed by iterative convolution of the luminescence decay profile with the instrument response function using software provided by Edinburgh Instruments.

Emission lifetimes were also measured with a nitrogen-pumped broadband dye laser (2−3 nm fwhm) from PTI (GL-3300 N_2 laser, GL-301 dye laser). The N_2 fundamental (337.1 nm) as well as Coumarin 460 (440−480 nm) and BPBD (350−400 nm) dyes were used to tune the unfocused excitation. Pulse energies were typically attenuated to ∼ 100 μJ/pulse, measured with a Molectron Joulemeter (J4-05). The luminescence was gathered at 90° through a long pass optical filter (550 nm), focused through a lens system, and passed through a *f*/3.4 monochromator (±4 nm). The emission was detected with a Hamamatsu R928 PMT, mounted in a Products for Research housing. The base of the PMT was wired for fast response and was negatively biased with a Stanford Research PS325 power supply. The PMT signal was terminated through a 50 ohm resistor to a Tektronix TDS 380 digital oscilloscope (400 MHz). The data from the scope, representing an average of 128 laser shots collected at 2−3 Hz, was transferred to a computer and processed using Origin 4.1.

Nanosecond time-resolved absorption spectroscopy was performed using instrumentation that has been described previously.[14] The excitation source was the unfocused second harmonic output (532 nm, 7 ns fwhm) of a Nd:YAG laser (Continuum Surelite I). The laser was typically attenuated to between 5 and 10 mJ/pulse prior to sample excitation. The probe lamp was filtered of all deep UV-output through the use of several long-pass filters in parallel (LP295, LP305, and LP350) prior to sample illumination. Samples were continuously purged with a stream of argon gas throughout the experiments. The data, consisting of a 10-shot average of both the signal and the

TABLE 1: Spectroscopic and Photophysical Data at Room Temperature in CH_3CN

complex	λ_{max}, nm (ϵ, $M^{-1}\,cm^{-1}$)	$\lambda_{em\ max}$, nm	τ_{em}, μs[a]	Φ_r[b]	$\tau(T-T_{abs})$, μs[c]	α[d]	K_{eq}[e]
$[Ru(dmb)_3]^{2+}$	458 (16 300)	622	0.875 ± 0.04	0.071 ± 0.008		0	0
$[Ru(dmb)_2(bpy\text{-}pyrene)]^{2+}$	343 (40 000), 459 (15 000)	621	2.96 ± 0.17	$0.065 + 0.007$	3.38 ± 0.40	0.64	1.8
$[Ru(bpy\text{-}pyrene)_3]^{2+}$	343 (91 800), 460 (14 600)	617	9.00 ± 0.14	0.064 ± 0.012	8.6 ± 0.80	0.87	6.7
bpy-pyrene	342 (37 000)	376, 397	0.246 ± 0.005[f]		100 ± 10[g]		

[a] Lifetimes represent an average of at least six measurements and have an uncertainty of less than 5%. Here the data were obtained using 458 $\pm$ 2 nm excitation. [b] Error bars represent reproducibility within 2σ, including the uncertainty in the measurement of the standard. [c] The lifetime of the triplet−triplet pyrene absorption, measured at 410 nm with 532 nm excitation. [d] The fraction of pyrene-like triplets in the excited-state equilibrium, measured by actinometry. See text for details. [e] Excited-state equilibrium constants calculated from the data in Figure 5 using eq 2. [f] Measured by TCSPC with 343 nm excitation. [g] 355 nm excitation, transient absorption detected at 420 nm.

baseline, were analyzed with programs of local origin. The UV−vis spectra of each compound before and after transient absorption measurements were the same within experimental error, indicating no sample decomposition during the data acquisition.

All photophysical experiments used optically dilute solutions (OD = 0.09−0.11) prepared in spectroscopic grade CH_3CN (Burdick and Jackson). All luminescence samples in 1 cm^2 anaerobic quartz cells (Starna Cells) were deoxygenated with argon for at least 30 min prior to measurement. Radiative quantum yields (Φ_r) were measured relative to $[Ru(bpy)_3](PF_6)_2$ for which $\Phi_r = 0.062$ in CH_3CN, accurate to 10%,[15] and calculated according to the following equation[13,16]

$$\Phi_{unk} = \Phi_{std}\left(\frac{I_{unk}}{A_{unk}}\right)\left(\frac{A_{std}}{I_{std}}\right)\left(\frac{\eta_{unk}}{\eta_{std}}\right)^2 \qquad (1)$$

where Φ_{unk} is the radiative quantum yield of the sample, Φ_{std} is the radiative quantum yield of the standard, I_{unk} and I_{std} are the integrated emission intensities of the sample and standard, respectively, A_{unk} and A_{std} are the absorbances of the sample and standard, respectively, at the excitation wavelength (458 nm), and η_{unk} and η_{std} are the indexes of refraction of the sample and standard solutions, respectively.

Results and Discussion

The ligand 4-methyl-4′-(2-hydroxyethylpyrenyl)-2,2′-bipyridine (bpy-pyrene) was prepared by the generation of the monocarbanion of commercially available 4,4′-dimethyl-2,2′-bipyridine (dmb) with LDA, followed by reaction with pyrenecarboxaldehyde, which generates the alcohol-containing ethane tether. Since the ligand and its Ru(II) complexes exhibited the desired photophysical properties, no further chemical elaboration of the ligand was performed. The dyad and tetrad complexes, $[Ru(dmb)_2(bpy\text{-}pyrene)]^{2+}$ and $[Ru(bpy\text{-}pyrene)_3]^{2+}$, respectively, were prepared according to standard procedures with final purification achieved through reversed-phase HPLC. $[Ru(dmb)_3]^{2+}$, prepared as a model system for the dyad and tetrad, was synthesized as described in the literature.[13]

The spectroscopic and photophysical data for the compounds in this study are displayed in Table 1. Shown in Figure 1a are the absorption spectra of bpy-pyrene and $[Ru(dmb)_3]^{2+}$ in CH_3CN. Figure 1b displays the absorption spectra of $[Ru(dmb)_2(bpy\text{-}pyrene)]^{2+}$ and $[Ru(bpy\text{-}pyrene)_3]^{2+}$ in CH_3CN. Both $[Ru(dmb)_2(bpy\text{-}pyrene)]^{2+}$ and $[Ru(bpy\text{-}pyrene)_3]^{2+}$ possess absorption bands that can only be attributed to contributions from the $[Ru(dmb)_3]^{2+}$ fragment and from the pyrenyl group(s). This suggests that there is no significant electronic interaction between the chromophores. The fact that the pyrene molecule(s) and the Ru(II) complex are weakly coupled is important for the discussion later on. In two of the four Ru(II)−pyrene systems that have been investigated in the literature,[4,5] there are indications that the molecules are strongly coupled,

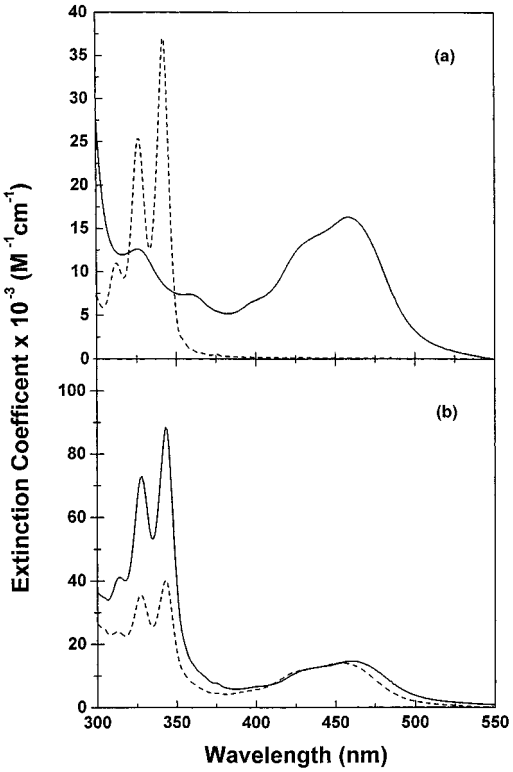

Figure 1. (a) Electronic spectra of $[Ru(dmb)_3]^{2+}$ (solid line) and bpy-pyrene (dashed line) in CH_3CN. (b) Electronic spectra of $[Ru(bpy\text{-}pyrene)_3]^{2+}$ (solid line) and $[Ru(dmb)_2(bpy\text{-}pyrene)]^{2+}$ (dashed line) in CH_3CN.

and behave more like supermolecules rather than as two individual units. Since the lowest energy pyrene bands are well removed from the $[Ru(dmb)_3]^{2+}$ transitions, good photoselectivity in this wavelength region can be achieved. In the dyad case, the pyrene chromophore accounts for ~79% of the light absorbed at 343 nm, whereas pyrene absorbs ~91% of the light at 343 nm in the tetrad. The enhanced absorption cross-sections between 300 and 350 nm from the pyrenyl chromophores provide an antenna system for the efficient harvesting of UV light (Scheme 1).

The luminescence spectrum of the free bpy-pyrene ligand in CH_3CN shows an intense emission band in the blue region of the spectrum (Figure 2), characteristic of the pyrene chromophore.[17] The lifetime of this emission was determined to be 246 ns in CH_3CN by TCSPC with 343 nm excitation. This luminescence band is almost quantitatively quenched when the ligand is chelated to Ru(II) in both the dyad and the tetrad (Figure 2). The quenching of the singlet pyrene emission is a result of highly efficient energy transfer to the $[Ru(bpy)_3]^{2+}$ chromophore. The corrected excitation and uncorrected luminescence spectra for the MLCT-based emission of $[Ru(dmb)_2(bpy\text{-}pyrene)]^{2+}$ and $[Ru(bpy\text{-}pyrene)_3]^{2+}$ in CH_3CN are pre-

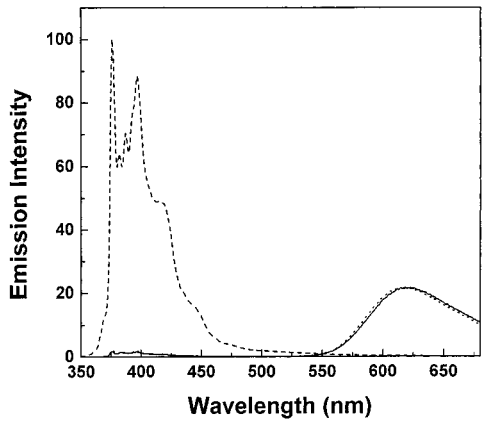

Figure 2. Emission spectra of bpy-pyrene (dashed line), $[Ru(dmb)_2(bpy\text{-}pyrene)]^{2+}$ (solid line), and $[Ru(bpy\text{-}pyrene)_3]^{2+}$ (dotted line) of optically matched solutions (0.10 OD) in deaerated CH_3CN. The excitation wavelength was 343 ± 2 nm.

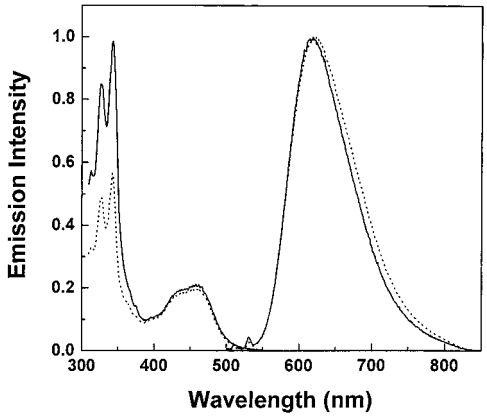

Figure 3. Corrected excitation and uncorrected emission spectra of $[Ru(bpy\text{-}pyrene)_3]^{2+}$ (solid lines) and $[Ru(dmb)_2(bpy\text{-}pyrene)]^{2+}$ (dotted lines) in CH_3CN at 25 °C. The excitation spectra were detected at 610 nm.

SCHEME 1

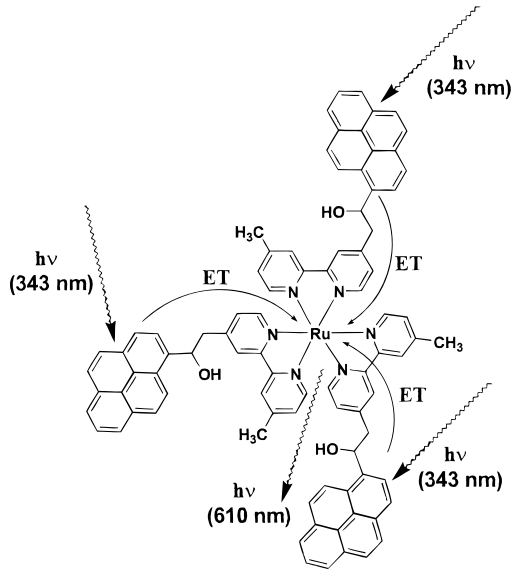

sented in Figure 3. The emission spectra are normalized to their respective peak wavelengths. The absorption spectrum and the excitation spectrum of the dyad are superimposable, suggesting the singlet−singlet energy transfer efficiency between the pyrenyl group(s) and the $[Ru(bpy)_3]^{2+}$ fragment in this system approaches unity.[18] This result is not surprising as similar observations have been previously made in other ethane-bridged Ru(II)−pyrene bichromophores.[3] In the tetrad case there is substantial overlap between the excitation and absorption spectra; however, they are not completely superimposable. In an attempt to further quantify the singlet−singlet energy transfer efficiency in the tetrad, we employed the TCSPC technique to the weak pyrene emission bands (near 400 nm) arising from direct excitation into the absorption at 343 nm. This residual emission displayed a lifetime of approximately 3.5 ns. On the basis of this value and the fluorescence lifetime of the free pyrenyl ligand, the energy transfer efficiency for the tetrad system is calculated to be 98.6%.[8a,19] The significant UV absorption cross-sections provided by the pyrenyl units along with the efficient energy transfer to the MLCT core allow dilute solutions (10^{-6}−10^{-7} M) of the tetrad to exhibit strong visible emission with UV excitation.

Excitation at wavelengths between 337.1 and 532 nm generates MLCT-based emission in both the dyad and tetrad complexes. In all experiments employed, the rise time of the MLCT-based emission could not be resolved, demonstrative of the fast rate of singlet energy transfer from pyrene to the Ru(II) core ($>10^9$ s^{-1}).[3b] The MLCT-based emission in both the dyad and tetrad are single exponential, with lifetimes of 2.96 and 9.0 μs, respectively, regardless of excitation wavelength.

The transient absorption spectra of the dyad and tetrad complexes following visible excitation at 532 nm are identical within experimental error. For brevity, only the tetrad's transient spectrum is displayed (Figure 4a). The spectra are characterized by a strong absorption at 405 nm and a weaker one near 515 nm that can be assigned to the triplet−triplet absorption of the pyrene chromophore.[2,3] There is no bleaching of the transient absorption spectrum in the 400−500 nm region at all delay times, indicating that the excitation energy is localized on the pyrene unit(s). Figure 4b displays the absorption transient of $[Ru(bpy\text{-}pyrene)_3]^{2+}$ at 410 nm following 532 nm pulsed excitation. The rise time of the pyrene triplet−triplet absorption could not be resolved with this instrumentation (<15 ns), indicating a fast triplet−triplet energy transfer from the $[Ru(bpy)_3]^{2+}$ unit to the pyrene unit(s). The decay of the triplet−triplet pyrene absorption follows the same kinetics as the MLCT-based luminescence decays in the dyad and tetrad, suggesting the two processes are intimately coupled, Table 1.[2,3] In fact, dynamic quenching of the emission decay by the addition of dioxygen quenches the pyrene triplet−triplet absorption decay in a similar manner. Comparable effects have been demonstrated in related Ru(II)−pyrene bichromophore studies.[2]

Previous studies have shown that the nearly isoenergetic triplet states of the $[Ru(bpy)_3]^{2+}$ unit and the pyrene chromophore(s) allow an excited-state equilibrium to become established.[2,3] Since the room-temperature radiative rate of the $[Ru(bpy)_3]^{2+}$ chromophore is much greater than the pyrene radiative decay rate,[20] all of the energy is emitted through the $[Ru(bpy)_3]^{2+}$ unit.[3] As shown in earlier studies, the partitioning of the excitation energy between the ^{3}pyrene and the ^{3}MLCT states can be determined through actinometry.[3a,b,5] In such an experiment, the MLCT-based emission at time zero (I_0) is monitored, following 458 nm laser excitation of optically matched solutions of $[Ru(dmb)_3]^{2+}$, $[Ru(dmb)_2(bpy\text{-}pyrene)]^{2+}$ and $[Ru(bpy\text{-}pyrene)_3]^{2+}$ in deaerated CH_3CN (Figure 5). In each case, an identical number of MLCT excited states are promptly formed during the laser pulse. However, in the case of the dyad and tetrad, triplet−triplet energy transfer to the pyrenyl unit(s) quickly depopulates the ^{3}MLCT states, resulting in diminished

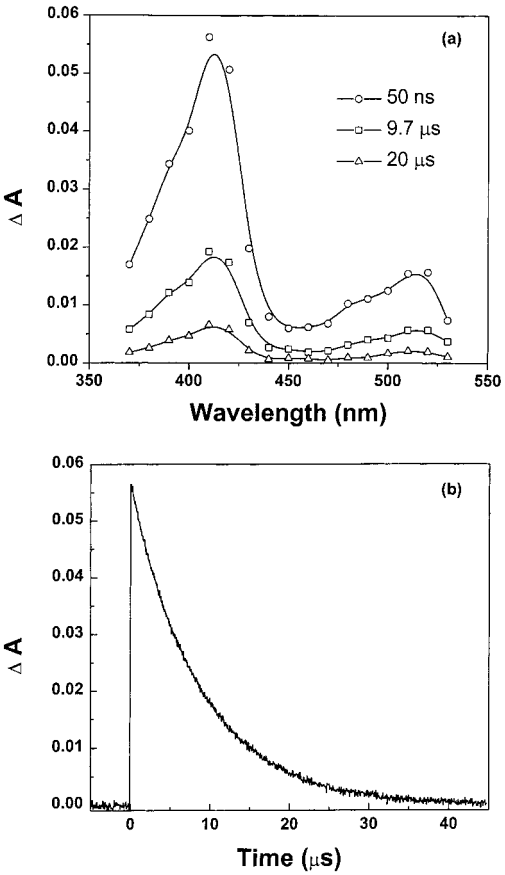

Figure 4. (a) Excited-state absorption difference spectra for [Ru(bpy-pyrene)$_3$]$^{2+}$ in deaerated CH_3CN recorded at 50 ns (open circles), 9.7 μs (open squares), and 20 μs (open triangles) following 532 nm pulsed excitation. (b) Time-resolved absorption kinetics of [Ru(bpy-pyrene)$_3$]$^{2+}$ in deaerated CH_3CN recorded at 410 nm following 532 nm laser excitation. The transient represents an average of 10 laser pulses.

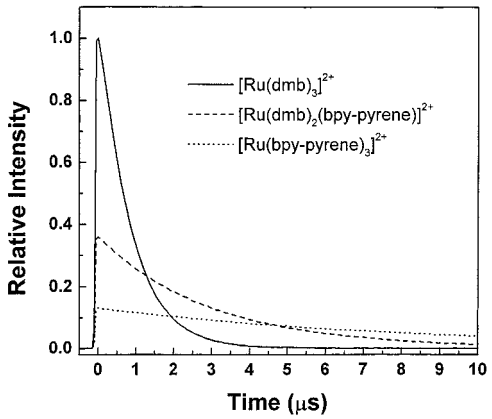

Figure 5. Time-resolved photoluminescence decays of [Ru(dmb)$_3$]$^{2+}$ (solid line), [Ru(dmb)$_2$(bpy-pyrene)]$^{2+}$ (dashed line), and [Ru(bpy-pyrene)$_3$]$^{2+}$ (dotted line) in deaerated CH_3CN obtained with 458 $\pm$ 2 nm pulsed excitation (500 ps fwhm) detected at 610 nm. Each decay represents an average of 128 laser pulses. The solutions were optically matched at 458 nm (0.10 OD).

emission intensity at time zero. In this experiment we assume the radiative decay rates for the ^{3}MLCT states in each complex are similar. Since the emission quantum yields are nearly the same for each complex (Table 1), this assumption is reasonable, and the data can be quantitatively assessed. It is also important to note that the equilibrium distribution is established faster than can be resolved with our instrumentation (<15 ns), and was established in less than 20 ps in a related dyad system.[5] Therefore, we cannot resolve the fast relaxation from the initial, nonequilibrium state and can only place limits on the actual forward triplet−triplet energy transfer rate constants in the present work.

The actinometry experiment measures the fraction of MLCT-based excited states at equilibrium in the dyad and tetrad, [Ru(bpy)$_3$]*$_{eq}$, using [Ru(dmb)$_3$]$^{2+}$ as the reference compound, Figure 5. The difference between the emission intensity for [Ru(dmb)$_3$]$^{2+}$ and the dyad or tetrad at time zero yields the fraction of pyrene-like triplets in the equilibrium distribution (α), making [Ru(bpy)$_3$]*$_{eq}$ equal to $1 - \alpha$. The value of the partition ratios can be used to calculate the excited-state equilibrium constant, K_{eq}, and the *relative* rates of triplet−triplet energy transfer between [Ru(bpy)$_3$]$^{2+}$ and the pyrene unit(s) using eq 2,[2,3,5]

$$K_{eq} = \frac{\alpha}{1-\alpha} = \frac{k_f}{k_r} \qquad (2)$$

where k_f is the rate of triplet energy transfer from the ^{3}MLCT states to the ^{3}pyrene states and k_r is the reverse process. For [Ru(dmb)$_2$(bpy-pyrene)]$^{2+}$, $\alpha = 0.64$ and $K_{eq} = 1.8$, whereas in [Ru(bpy-pyrene)$_3$]$^{2+}$, $\alpha = 0.87$ and $K_{eq} = 6.7$. The fraction of pyrene-like triplets (α) should be controlled by the energy gap between the ^{3}MLCT level and the ^{3}pyrene level and by the relative rates of k_f and k_r.[5] The MLCT emission profile in the dyad and tetrad are nearly superimposable and have similar emission onsets (Figure 3). The emission onset can be used to crudely estimate the ^{3}MLCT energy levels in the two molecules.[1] Within our experimental error ($\pm$2 nm), there is no marked difference in the ^{3}MLCT energy of the dyad and tetrad complexes. The pyrene triplet is formed on the same ligand (bpy-pyrene) in both cases so the pyrene triplet energy should remain the same in both complexes. The triplet−triplet absorption spectra following visible excitation in both complexes are identical, suggesting that this is a reasonable assumption. Since the ^{3}MLCT and the ^{3}pyrene energy levels are constant in the dyad and tetrad, the increase in K_{eq} in the tetrad cannot be explained by a variation in energy gap. The rate constant for back triplet transfer, k_r, is not expected to change between the dyad and tetrad because the recombination always occurs to a single Ru(II) complex. However, k_f will increase as the number of triplet acceptors increase. The dyad has one pyrene and the tetrad contains three pyrene molecules, so one would expect an increase in k_f (and K_{eq}) in going from the former to the latter, as long as k_r remains constant. The measured 3.7-fold increase in K_{eq} in the tetrad results in a 3-fold enhancement of the observed emission and triplet lifetimes (Table 1). This result implies that driving the excited-state equilibrium to the right (favoring ^{3}pyrene) will lead to an observation of enhanced ^{3}MLCT and ^{3}pyrene lifetimes in this class of molecules. Therefore, increasing k_f through the use of multiple triplet acceptors allows the emission lifetimes to be extended in a predictable way. A qualitative energy level diagram representing the relevant photophysical processes occurring in the dyad and tetrad are summarized in Figure 6.

Conclusions

The present work takes advantage of two characteristics of Ru(II)−pyrene chromophores. On one hand, multiple pyrene chromophores allow for the efficient harvesting of UV photons to sensitize MLCT excited state formation by using the antenna effect and singlet−singlet energy transfer processes. UV excitation of dilute solutions of the tetrad (10^{-6}−10^{-7}M) yields a strong visible MLCT-based emission. These results suggest the

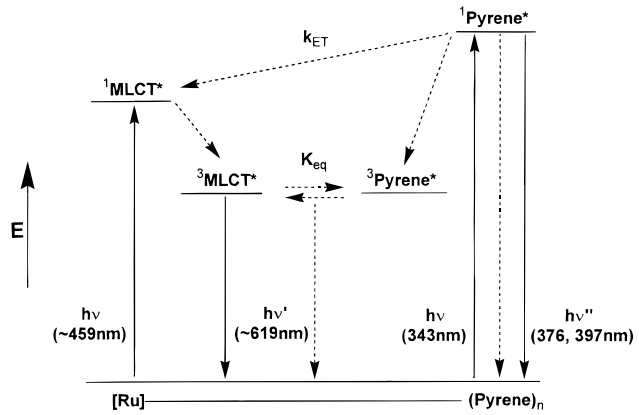

Figure 6. Qualitative energy level diagram describing the photophysical processes of $[Ru(bpy\text{-}pyrene)_3]^{2+}$ and $[Ru(dmb)_2(bpy\text{-}pyrene)]^{2+}$. Solid lines represent radiative transitions and dashed lines represent nonradiative transitions.

singlet−singlet energy transfer strategies traditionally employed in artificial light-harvesting arrays can be adapted to incorporate MLCT compounds as *acceptors*. The sensitized ^{3}MLCT emissive states are in rapid thermal equilibrium with the triplet states of the pyrene molecule(s). The excited-state equilibrium constants and triplet lifetimes are modulated by the fractional contributions of each individual triplet molecule involved in the equilibrium (^{3}pyrene and ^{3}MLCT). Synthetic control of the luminescence lifetime is possible in such molecules by simply changing the number of pyrenyl triplet acceptor units. The prolongation of MLCT lifetimes is valuable for the advancement of analytical luminescence-based technologies such as lifetime-based sensing.[8,21]

Acknowledgment. The authors would like to thank Prof. M. A. J. Rodgers and Prof. G. S. Hammond for several helpful discussions and Dr. K. Henbest for his help with the transient absorption measurements.

References and Notes

(1) For reviews of MLCT excited states: (a) Juris, A.; Balzani, V.; Barigellitti, F.; Campagna, S.; Belser, P.; VonZelewsky, A. *Coord. Chem. Rev.* **1988**, *84*, 85. (b) Meyer, T. J. *Acc. Chem. Res.* **1989**, *22*, 1048. (c) Demas, J. N.; DeGraff, B. A *Anal. Chem.* **1991**, *63*, 829A. (d) Kalyanasundaram, K. *Photochemistry of Polypyridine and Porphyrin Complexes*; Academic Press: San Diego, CA, 1992. (e) Roundhill, D. M. *Photochemistry and Photophysics of Metal Complexes*; Plenium Press: New York, 1994. (f) Ramamurthy, V., Schanze, K. S., Eds. *Organic and Inorganic Photochemistry*; M. Dekker: New York, 1998.

(2) Ford, W. E.; Rodgers, M. A. J. *J. Phys. Chem.* **1992**, *96*, 2917.

(3) (a) Wilson, G. J.; A.; Sasse, W. H. F.; Mau, A. W. H *Chem Phys. Lett.* **1996**, *250*, 583. (b) Wilson, G. J.; Launikonis, A.; Sasse, W. H. F.; Mau, A. W. H. *J. Phys. Chem. A* **1997**, *101*, 4860. C) Wilson, G. J.; Launikonis, A.; Sasse, W. H. F.; Mau, A. W. H.. *J. Phys. Chem. A* **1998**, *102*, 5150.

(4) Simon, J. A.; Curry, S. L.; Schmehl, R. H.; Schatz, T. R.; Piotrowiak, P.; Jin, X.; Thummel, R. P. *J. Am. Chem. Soc.* **1997**, *119*, 11012.

(5) Harriman, A.; Hissler, M.; Khatyr, A.; Ziessel, R. *J. Chem. Soc. Chem. Commun.* **1999**, 735.

(6) Tyson, D. S.; Castellano, F. N. *Inorg. Chem.* **1999**, *38*, 4382.

(7) Plevoets, M.; Vogtle, F.; DeCola, L.; Balzani, V. *New J. Chem.* **1999**, *23*, 63.

(8) (a) Lakowicz, J. R. *Principles of Fluorescence Spectroscopy*, 2nd ed.; Kluwer Academic/Plenum Publishers: New York, 1999. (b) *Topics in Fluorescence Spectroscopy, Vol. 4: Probe Design and Chemical Sensing*; Lakowicz, J. R., Ed.; Plenum Press: New York, 1994.

(9) Balzani, V.; Scandola, F. *Supramolecular Photochemistry*; Horwood: Chichester, England, 1991.

(10) Lehn, J.-M. *Supramolecular Chemistry: Concepts and Perspectives*, VCH: Weinheim, Germany, 1995.

(11) Sullivan, B. P.; Salmon, D. J.; Meyer, T. J. *Inorg. Chem.* **1978**, *17*, 3334.

(12) Evans, I. P.; Spencer, A.; Wilkinson, G. *J. Chem. Soc., Dalton Trans.* **1973**, 204.

(13) Damrauer, N. H.; Boussie, T. R.; Devenney, M.; McCusker, J. K. *J. Am. Chem. Soc.* **1997**, *119*, 8253.

(14) (a) Mulazzani, Q. G.; Sun, H.; Hoffman, M. Z.; Ford, W. E.; Rodgers, M. A. J. *J. Phys. Chem.* **1994**, *98*, 1145. (b) Zhang, X.; Rodgers, M. A. J. *J. Phys. Chem.* **1995**, *99*, 12797.

(15) Casper, J. V.; Meyer, T. J. *J. Am. Chem. Soc.* **1983**, *105*, 5583.

(16) Demas, J. N.; Crosby, G. A. *J. Phys. Chem.* **1971**, *75*, 991.

(17) Berlman, I. B. *Handbook of Fluorescence Spectra of Aromatic Molecules*, 2nd ed.; Academic Press: New York, 1971.

(18) Devadoss, C.; Bharathi, P.; Moore, J. S. *J. Am. Chem. Soc.* **1996**, *118*, 9635. (b) Shortreed, M. R.; Swallen, S. F.; Shi, Z. Y.; Tan, W.; Xu, Z, Devadoss, C.; Moore, J. S.; Kopelman, R. *J. Phys. Chem. B* **1997**, *101*, 6318.

(19) Turro, N. J. *Modern Molecular Photochemistry;* Benjamin/Cummings: Menlo Park, CA, 1978; Chapter 9.

(20) Langelaar, J.; Rettschnick, R. P. H.; Hoijtink, G. J. *J. Chem. Phys.* **1971**, *54*, 1.

(21) Szmacinski, H.; Lakowicz, J. R. *Sensors Actuators B* **1995**, *29*, 16. (b) Castellano, F. N.; Lakowicz, J. R. *Photochem. Photobiol.* **1998**, *67*, 179. (c) Lakowicz, J. R.; Castellano, F. N.; Dattelbaum, J. D.; Tolosa, L.; Rao, G.; Gryczynski, I. *Anal. Chem.* **1998**, *70*, 5115.